

## Recent results of Daya Bay Experiment

Dongmei Xia<sup>1,a</sup>, on behalf of the Daya Bay Collaboration

<sup>1</sup> College of Power Engineering, Chongqing University, Chongqing 400044, China

**Abstract.** The Daya Bay reactor neutrino experiment aimed to precisely measure the least known mixing angle  $\theta_{13}$ . In March 2012, Daya Bay announced the non-zero value with more than  $5\sigma$ . With more statistics, less background and better control of systematics, the Daya Bay experiment is continuously improving the precision of  $\sin^2 2\theta_{13}$  as well as the effective neutrino mass squared differences. In this paper, I will report the recent oscillation results, which are the most precise measurement of the oscillation parameter  $\theta_{13}$  and  $|\Delta m_{ee}^2|$ . With 1230 days of data,  $\sin^2 2\theta_{13}$  is measured to be  $[8.41 \pm 0.27(\text{stat.}) \pm 0.19(\text{syst.})] \times 10^{-2}$ , and  $|\Delta m_{ee}^2| = [2.50 \pm 0.06(\text{stat.}) \pm 0.06(\text{syst.})] \times 10^{-3} \text{eV}^2$  with  $\chi^2/\text{NDF} = 232.6/263$ . An independent measurement with the inverse beta decay neutron captured on hydrogen will also be presented.

### 1 Introduction

Using the PMNS matrix  $U_{\text{PMNS}}$ , a neutrino with flavor  $\alpha$  can be expressed as a combination of the mass eigenstates of neutrino.

$$\nu_\alpha = \sum_i U_{\alpha i} \nu_i, \quad (1)$$

where  $\alpha = e, \mu, \tau$  for flavor eigenstates, and  $i = 1, 2, 3$  for mass eigenstates. In the three-flavor model,  $U_{\text{PMNS}}$  is commonly parameterized with three mixing angles ( $\theta_{12}$ ,  $\theta_{23}$ , and  $\theta_{13}$ ) and the CP-violating phase  $\delta_{CP}$ . Of these mixing angles,  $\theta_{13}$  is the least known. Solar and long baseline reactor experiments have measured  $\theta_{12}$  [1, 2] and atmospheric and accelerator experiments measured  $\theta_{23}$  [3, 4].

Previous short baseline reactor and accelerator neutrino experiments found no evidence of reactor antineutrino disappearance, but limited the value of  $\theta_{13}$  to be less than 10 degree at 90% confidence level. The remain unknowns in neutrino oscillation include the mass hierarchy of neutrino and the CP phase. A non-zero value for  $\theta_{13}$  makes it possible to measure the unknowns. And the magnitude of  $\theta_{13}$  is the signpost for future experiments to determine the neutrino mass hierarchy and to search for neutrino CP-violation.

The reactor antineutrino survival probability can be expressed using

$$P_{\bar{\nu}_e \rightarrow \bar{\nu}_e}(L) = 1 - \cos^4 \theta_{13} \sin^2 2\theta_{12} \sin^2 \Delta_{21} - \sin^2 2\theta_{13} \left( \cos^2 \theta_{12} \sin^2 \Delta_{31} + \sin^2 \theta_{12} \sin^2 \Delta_{32} \right), \quad (2)$$

where  $\sin^2 \Delta_{ee} \equiv \cos^2 \theta_{12} \sin^2 \Delta_{31} + \sin^2 \theta_{12} \sin^2 \Delta_{32}$ . KamLAND experiment measured  $\theta_{12}$  with an effective baseline of about 180 km [2]. For short baseline reactor experiments,  $\Delta_{31}$  and  $\Delta_{32}$  are indistinguishable, therefore, Eq. (2) can be approximately expressed with a single effective parameter  $\sin^2 \Delta_{ee}$ .

---

<sup>a</sup>e-mail: xiadm@cqu.edu.cn

Previous searches of  $\theta_{13}$  with reactor neutrinos were limited by uncertainty from reactors. A far versus near relative measurement can offset this uncertainty.

$$\frac{N_f}{N_n} = \left( \frac{N_{p,f}}{N_{p,n}} \right) \left( \frac{L_n}{L_f} \right)^2 \left( \frac{\epsilon_f}{\epsilon_n} \right) \frac{P_{sur}(E_\nu, L_f)}{P_{sur}(E_\nu, L_n)}. \quad (3)$$

Of this method, sensitivity to neutrino oscillation depends on relative uncertainties between detectors, including the number of target protons  $N_p$ , the baselining  $L$  and the detecting efficiency. Three experiments were constructed based on this technique, Daya Bay [5], RENO [6], and Double CHOOZ [9]. In March 2012, Daya Bay reported the discovery of the non-zero  $\theta_{13}$  [5], and then be confirmed by the other two experiments [6, 9]. The large value of  $\theta_{13}$  has allowed the measurement of  $\Delta m_{ee}$  from the oscillation of the neutrino energy spectrum.

## 2 The Daya Bay Experiment

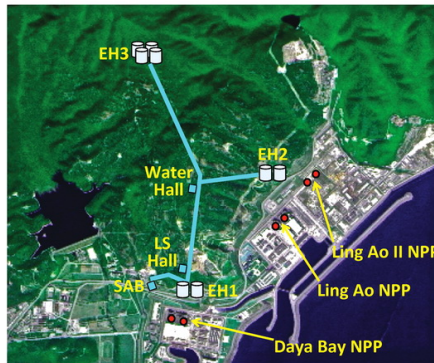


**Figure 1.** Layout of the Daya Bay Experiment.

The experiment is located in the Daya Bay nuclear power station in ShenZhen, which is in the south of China, and about 55 km away from Hong Kong. Figure 1 shows the layout of the experiment. There are 6 reactor cores with a total power of 17.4  $GW_{th}$  (giga wats), and three experimental halls (The Daya Bay near site, LingAo near site and the far site) with 8 operating detectors, the total target mass of the detectors is 160 ton. The coordinates of each detector and reactor can be found in [19]. The e coordinates were detected using GPS, and the uncertainties of the coordinates were 18mm. Details of the experimental layout can be found in [10].

In the experimental hall, a water cerenkov detector and the resistive plate chambers are used to tag muons, two identical designed antineutrino detectors(AD) are mounted in each near experimental hall, and 4 identical ADs were mounted in the far hall [17].

Each AD is constructed as a nested three zone structure, as shown in Figure 2. The inner most is the 3-meter acrylic tank, containing 20 tons of gadolinium loaded liquid scintillator(GdLS), which is the antineutrino target. In the 4-meter acrylic tank, it contains 22 tons of normal liquid scintillator (LS), with a function of gamma catcher. The outermost is the buffer shielding. Three automatic calibration units (ACU-A, ACU-B, ACU-C) were mounted on the top of each AD for detector calibration. 192 PMTs are used to collect photons. Details of the antineutrino detector can refer to [17]

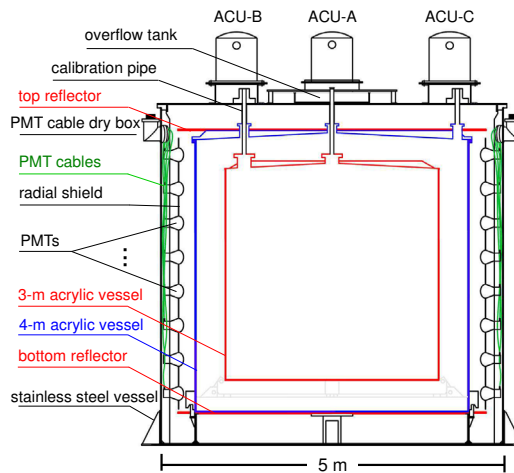


**Figure 2.** Scheme of the antineutrino detector.

The experiment started the data taking in Dec 2011, with the operating of 6 AD. The 8AD data taking period started in October 2012. Last year, we published the 621 days data result which combined the 6-AD and 8-AD period data [10], and the 1230 days data result will be published soon.

### 3 Energy Calibration

To do the energy calibration, the first step is to do the PMT gain calibration. There are two methods for PMT gain calibration, one is based on the single photoelectron from the PMT dark noise, and the other is based on the weekly deployment of LED. The second step is the energy calibration, both the calibration sources as well as the spallation neutrons were used for energy calibration.

The AD-to-AD relative energy scale was also measured using 13 different calibration sources, including both deployed and naturally occurred sources. The calibration sources include  $^{68}\text{Ge}$ ,  $^{60}\text{Co}$  and AmC neutron sources; Neutrons from IBD and muon spallation captured both on H and Gd were used. Signals generated by natural radioactivity including  $\alpha$  decays and  $\gamma$  rays from  $^{40}\text{K}$  and  $^{208}\text{Tl}$  were also compared between detectors. Figure 3 shows the comparison of the mean reconstructed energy between the ADs for these 13 various sources. Error bars in the figure are statistical only, and relative energy scale uncertainty for all calibration sources were less than 0.2%. The 8 MeV n-Gd capture  $\gamma$  peaks from Am-C sources were used to define the energy scale of each detector.

The energy model of Daya Bay experiment include the nonlinearity from liquid scintillator and the readout electronics. The energy model was built based on various  $\gamma$  peaks and continuous  $^{12}\text{B}$  beta spectrum. This model was also validated using independent calibration data, include the Michel electron, the  $\beta+\gamma$  continuous spectra from Bi and Tl decays, and the Compton scattering electron data. Figure 4 shows the energy model, which the uncertainty band corresponds to the model consistent with the calibration data within 68% C.L. The prominent nonlinearity below 4 MeV was attributed to scintillator light yield (from ionization quenching and Cherenkov light production) and the charge response of the electronics. Gamma rays from both deployed and intrinsic sources as well as spallation  $^{12}\text{B}$  decay determined the energy model, and provided an envelope of curves consistent with the data within a 68.3% C.L. (grey band). An independent estimate using the  $\beta+\gamma$  energy spectra from  $^{212}\text{Bi}$ ,

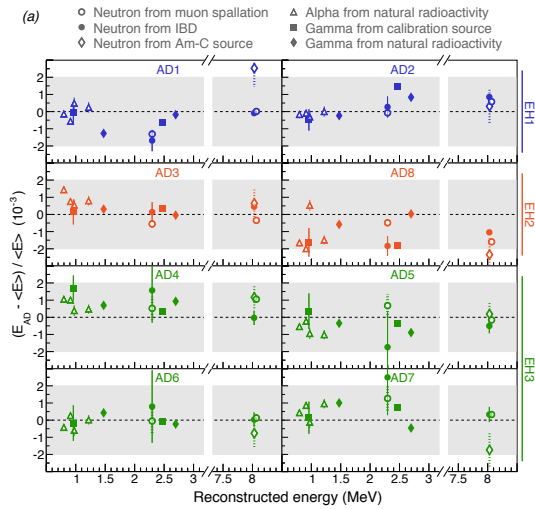


**Figure 3.** Comparison of the reconstructed energy between antineutrino detectors for a variety of calibration references.  $E_{AD}$  is the reconstructed energy determined using each AD, and  $\langle E \rangle$  is the 8-detector average.

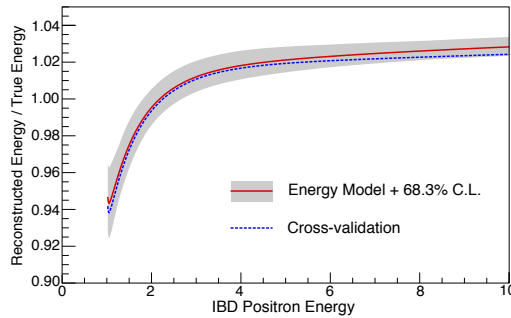


**Figure 4.** Estimated energy response of the detectors to positrons, including both kinetic and annihilation gamma energy (red solid curve).

$^{214}\text{Bi}$ ,  $^{208}\text{Tl}$ , and the 53-MeV edge in the Michael electron spectrum gave a similar result (blue dashed line), with larger systematic uncertainties [10].

## 4 Event selection

Antineutrinos are detected via inverse beta decay (IBD), which provides two time-correlated signals of specific energies. The first, or prompt signal is produced by positron. The delayed signal is neutron, which can be captured on Gd or H. If it was captured on Gd, the capture time is about 30  $\mu\text{s}$ , and the excited Gd will release  $\sim 8\text{MeV}$  of  $\gamma$  rays. If it was captured on H, the capture time is about 200 $\mu\text{s}$ , and releasing  $\sim 2.2\text{MeV}$   $\gamma$  rays.

To select IBD events, the PMT flashers are removed which are instrumental backgrounds[11]. Then the coincidence cut is applied, with the prompt energy between 0.7 and 12 MeV, the delayed energy between 6 and 12MeV. The coincidence time cut was applied as more than 1us and less than 200us. The combined efficiency was estimated to be 80.6%. The absolute efficiencies and their correlated uncertainties were canceled when comparing the ratio of signals in the far versus near detectors. Therefore, only the uncorrelated uncertainties were considered. The uncorrelated uncertainty of detection efficiency was estimated to be 0.13% [10].

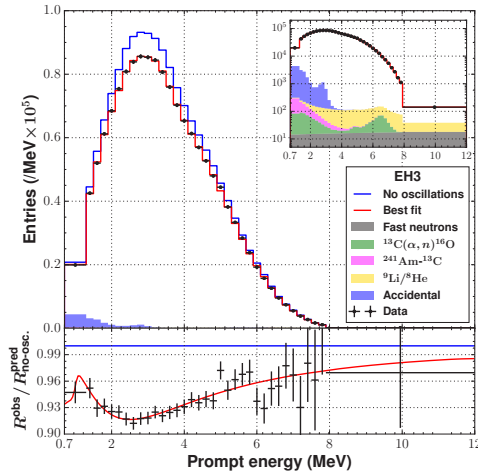


**Figure 5.** (upper) The observed reconstructed positron energy spectrum for EH3(black points), compared with the prediction assuming no oscillation (blue line) and the best three-flavor neutrino oscillation model (red line). (Lower) The ratio of the background-subtracted spectra to the prediction assuming no oscillation.

There are five main backgrounds including the accidentals, the fast neutrons, the  ${}^9\text{Li}/{}^8\text{He}$ ,  ${}^{13}\text{C}(\alpha,n){}^{16}\text{O}$ , and the background from the calibration source  ${}^{241}\text{Am}-{}^{13}\text{C}$ . The uncertainty of these backgrounds were limited to  $\leq 0.2\%$  for each experimental hall. In summary, the backgrounds were estimated to contribute 1.8% to the sample from EH1, 1.5% to EH2, and 2.0% to EH3. And the uncertainties of background were 0.2%, 0.15% and 0.2% for the three experimental hall, respectively. The upper panel of Figure 5 shows the positron energy spectra distribution in EH3, and compared the experimental data to prediction assuming no oscillation. The estimated background are barely visible as can be seen from the figure. The ratios of the data to predictions assuming no oscillation are shown in the lower panel of figure 5, to highlight the spectral distortion. The distortion of the energy spectra is consistent with oscillation, which allowed to measure  $\Delta m_{ee}$ .

With the 1230 days of data, over 2.8 million IBD candidates were obtained. This is double statistics of the result we published with 621 days data in 2015. Figure 6 shows the survival probability versus L/E for the three experimental hall using the 1230 days of data. The points are the ratios of the observed antineutrino spectra to expectation assuming no oscillation. The solid line is the expectation using the best estimates of the two parameters,  $\sin^2 2\theta_{13}$  and  $|\Delta_{ee}|$ . Error bars are statistical only.  $\langle E_\nu \rangle$  was obtained using the estimated detector response, while  $L_{eff}$  was calculated by equating the actual

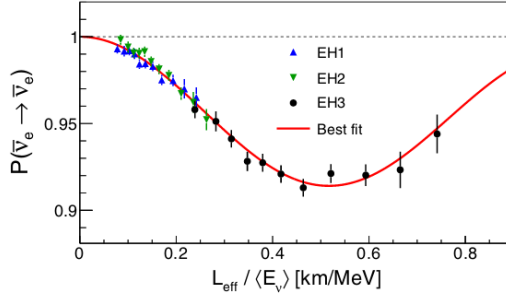


**Figure 6.** Electron antineutrino survival probability versus effective propagation distance  $L_{eff}$ , divided by the average antineutrino energy  $\langle E_\nu \rangle$ .

flux to an effective antineutrino flux using a single baseline. And all the three experimental halls were consistent with the oscillation hypothesis.

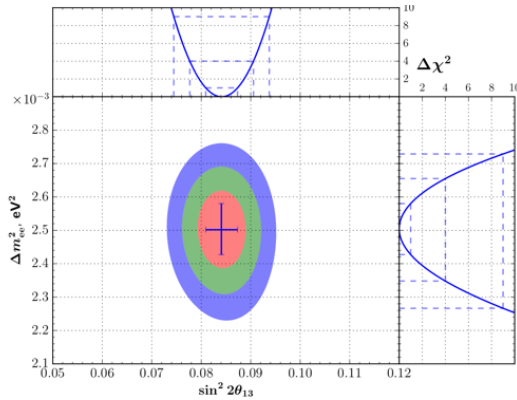
## 5 Oscillation results

Figure 7 shows the 2-D confidence and the  $\Delta\chi^2$  versus  $\Delta m_{ee}$  and  $\sin^2 2\theta_{13}$ . The upper panel shows the 1-D confidence of  $\theta_{13}$  when profiling  $\Delta m_{ee}$ , and the right panel gives the 1-D confidence of  $\Delta m_{ee}$  when profiling  $\theta_{13}$ . The best fit gives the central value of  $\theta_{13}$  and  $\Delta m_{ee}$ .

$$\sin^2 2\theta_{13} = [8.41 \pm 0.27(stat.) \pm 0.19(syst.)] \times 10^{-2}, \quad (4)$$

$$|\Delta m_{ee}^2| = [2.50 \pm 0.06(stat.) \pm 0.06(syst.)] \times 10^{-3} \text{eV}^2, \quad (5)$$

$$\chi^2/NDF = 232.6/263. \quad (6)$$



**Figure 7.** Confidence intervals for  $\sin^2 2\theta_{13}$  and  $|\Delta m_{ee}^2|$  from comparison of the antineutrino rate and prompt positron spectra observed in the far versus near detectors.

With the 1230 days of data, Daya Bay experiment gives the most precise measurement of both  $\theta_{13}$  and  $\Delta m_{ee}$ . And the result is consistent with the MeV-scale reactor experiments like RENO [7],

Double CHOOZ[8], and consistent with the GeV-scale accelerator experiments like T2K[13], MINOS [12] and NOvA[14], and consistent with the atmospheric experiments like supreK [15] and Icecube [16].  $\Delta m_{32}^2$  is  $2.45 \times 10^{-3} eV^2$  when consider normal hierarchy. While  $-2.55 \times 10^{-3} eV^2$  when consider inverted mass hierarchy.

## 6 Independent measurement of $\theta_{13}$ using nH

An independent measurement of  $\sin^2 2\theta_{13}$  has been measured via the detection of IBDs tagged by neutron capture on hydrogen (nH) by Daya Bay experiment. The background of nH analysis is higher, the neutron capture time (200ms) is longer, and the energy neutron captured on hydrogen is lower (2.2MeV). To meet these challenges, new analysis approaches have been developed. Based on the rate deficit observed at the far-site detectors for the 6-AD period, a value of  $\sin^2 2\theta_{13} = 0.071 \pm 0.011$  is extracted. The result is shown in Figure 8, which is consistent with the result obtained in the nGd analysis. Details of the nH analysis can refer to [18]

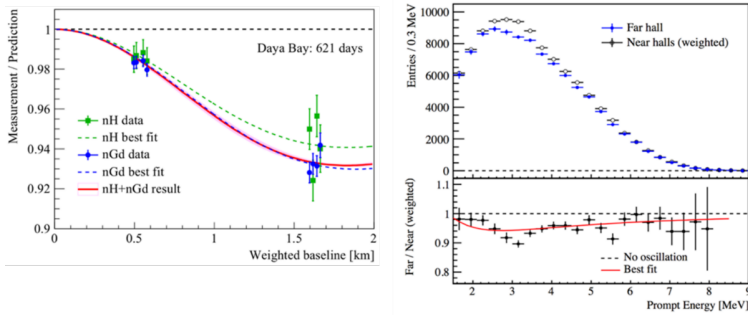


**Figure 8.** Left: Comparison of the nGd and nH analysis of the measurement over prediction assuming no oscillation versus weighted baseline, using 621 days of data. Right: The top panel shows the reconstructed prompt-energy spectrum of the far hall (solid blue points) and the expectation based on the measurements of the two near halls (empty black points). Spectra are background-subtracted. Error bars are purely statistical. The bottom panel shows the ratio of the Far/Near halls, and the curve representing the best value of  $\sin^2 2\theta_{13} = 0.071 \pm 0.011$ .

## 7 Summary

In this article, I present the latest results of the oscillation analysis from Daya Bay Experiment. With 1230 days of data, the most precise measurement of  $\sin^2 2\theta_{13}$  and  $|\Delta m_{ee}^2|$  are given

$$\begin{aligned} \sin^2 2\theta_{13} &= [8.41 \pm 0.33] \times 10^{-2}, \\ |\Delta m_{ee}^2| &= [2.50 \pm 0.08] \times 10^{-3} eV^2, \\ \Delta m_{32}^2(NH) &= [2.45 \pm 0.08] \times 10^{-3} eV^2, \\ \Delta m_{32}^2(IH) &= [-2.55 \pm 0.08] \times 10^{-3} eV^2. \end{aligned}$$

Independent measurement  $\sin^2 2\theta_{13}$  using neutron captured on hydrogen with 631-day of data is also presented.  $\sin^2 2\theta_{13} = 0.071 \pm 0.011$ .

## 8 Acknowledgments

Part of this work is supported by the National Natural Science Foundation of China (Grant No. 11505018) and Chongqing Science and Technology plan project (Grant No. Cstc2015jcyj40031). Daya Bay is supported in part by the Ministry of Science and Technology of China, the U.S. Department of Energy, the Chinese Academy of Sciences, the CAS Center for Excellence in Particle Physics, the National Natural Science Foundation of China, the Guangdong provincial government, the Shenzhen municipal government, the China General Nuclear Power Group, Key Laboratory of Particle and Radiation Imaging (Tsinghua University), the Ministry of Education, Key Laboratory of Particle Physics and Particle Irradiation (Shandong University), the Ministry of Education, Shanghai Laboratory for Particle Physics and Cosmology, the Research Grants Council of the Hong Kong Special Administrative Region of China, the University Development Fund of The University of Hong Kong, the MOE program for Research of Excellence at National Taiwan University, National Chiao-Tung University, and NSC fund support from Taiwan, the U.S. National Science Foundation, the Alfred P. Sloan Foundation, the Ministry of Education, Youth, and Sports of the Czech Republic, the Joint Institute of Nuclear Research in Dubna, Russia, the CNFCRFBR joint research program, the National Commission of Scientific and Technological Research of Chile, and the Tsinghua University Initiative Scientific Research Program. We acknowledge Yellow River Engineering Consulting Co., Ltd., and China Railway 15th Bureau Group Co., Ltd., for building the underground laboratory. We are grateful for the ongoing cooperation from the China General Nuclear Power Group and China Light and Power Company

## References

- [1] Q. R. Ahmad et al. (SNO Collaboration), *Phys. Rev. Lett.* 89,2676 011301 (2002).
- [2] S. Abe et al. (KamLAND Collaboration), *Phys. Rev. Lett.* 100,2678 221803 (2008).
- [3] Y. Fukuda et al. (Super-Kamiokande Collaboration), *Phys. Rev.*2670 Lett. 81, 1562 (1998).
- [4] M. H. Ahn et al. (K2K Collaboration), *Phys. Rev. Lett.* 90,2672 041801 (2003).
- [5] F. P. An et al. (Daya Bay Collaboration), *Phys. Rev. Lett.* 108,171803 (2012).
- [6] J. Ahn et al. (RENO Collaboration), *Phys. Rev. Lett.* 108,191802 (2012).
- [7] J. H. Choi et al. (RENO), *Phys. Rev. Lett.* 116, 211801 (2016).
- [8] M. Ishitsuka, “Double chooz,” (2016), moriond 2016.
- [9] Y. Abe (Double Chooz Collaboration), *Phys. Rev. Lett.* 108,131801 (2012).
- [10] F.P.An et al. (Daya Bay Collaboration), *Phys. Rev. Lett.* 115, 111802 (2015).
- [11] F.P.An et al. (Daya Bay Collaboration), *Nucl. Instr. Meth. A* 685, 78 (2012) .
- [12] P. Adamson et al. (MINOS Collaboration), *Phys. Rev. Lett.* 110,171801(2013).
- [13] K. Abe et al. (T2K), *Phys. Rev. D*91, 072010 (2015).
- [14] P. Adamson et al. (NOvA), *Phys. Rev. Lett.* 116, 151806 (2016).
- [15] R. Wendell (Super-Kamiokande), (2014), arXiv:1412.5234[hep-ex].
- [16] M. G. Aartsen et al. (IceCube), *Phys. Rev. D*91, 072004 (2015).
- [17] F. P. An et al. (Daya Bay Collaboration), *Chin. Phys. C* 37,011001 (2013).
- [18] F. P. An et al. (Daya Bay Collaboration), *Phys. Rev. D*90, 071101(2014).
- [19] F. P. An et al. (Daya Bay Collaboration), arXiv:1610.04802 [hep-ex].